Cl(20,I) qui se trouve à égale distance des deux C(12,VI) et C(12,II).

Conclusion

La structure cristalline du dichloroisoprotérénol se différencie nettement des composés de cette série des β bloquants (Gadret, Goursolle, Leger & Colleter, 1975). La différence essentielle réside dans la cristallisation dans un groupe orthorhombique. Par contre au niveau de la molécule elle-même, on retrouve sensiblement les mêmes caractéristiques en particulier pour la chaîne alkylaminée.

Références

COLLETER, J. C., GADRET, M., GOURSOLLE, M. & LEGER, J. M. (1974). Premier Congrès des Sociétés de Pharmacie, Nantes.

GADRET, M., GOURSOLLE, M., LEGER, J. M. & COLLETER, J. C. (1975). *Acta Cryst.* B**31**, 1938–1942.

GERMAIN, P., MAIN, P. & WOOLFSON, M. M. (1970). *Acta Cryst.* B**26**, 274–285.

LOPEZ DE LERMA, J., MARTÍNEZ-CARRERA, S. & GARCÍA BLANCO, S. (1973). *Acta Cryst.* B**29**, 537–541.

SCHOMAKER, V., WASER, J., MARSH, R. E. & BERGMAN, G. (1959). *Acta Cryst.* **12**, 600–604.

STEWART, R. F., DAVIDSON, E. R. & SIMPSON, W. T. (1965). *J. Chem. Phys.* **42**, 3175–3178.

Acta Cryst. (1975). B**31**, 1946

Hydrogen Bond Studies. XCVI.* X–N Maps and *ab initio* MO-LCAO-SCF Calculations of the Difference Electron Density in Non-Centrosymmetric Lithium Formate Monohydrate, $LiHCOO.H_2O$

BY JOHN O. THOMAS, ROLAND TELLGREN AND JAN ALMLÖF

Institute of Chemistry, Uppsala University, Box 531, *S*-751 21 *Uppsala, Sweden*

(*Received* 8 *November* 1974; *accepted* 18 *February* 1975)

Accurate X-ray and neutron diffraction data have been combined to study the electron distribution in non-centrosymmetric lithium formate monohydrate, $LiHCOO.H_2O$. *Ab initio* MO-LCAO-SCF calculations of the difference electron density have also been made using a Gaussian basis set in which an arrangement of point charges has been taken to simulate the effect of the crystal field. Both techniques indicate a significant dissimilarity in the electron density distributions associated with the two O–H bonds of the water molecule. It also emerges from the *ab initio* calculations that the inclusion of the polarizing effect of the crystal environment is essential if agreement with experimental observation is to be achieved.

Introduction

This is the first of a series of systematic X–N difference electron density studies of the water molecule in simple hydrates, the general purpose being to examine the (difference) electron distribution associated with the water molecule in different hydrogen-bond environments. In the non-centrosymmetric structure lithium formate monohydrate, $LiHCOO.H_2O$, previous investigations have provided irrefutable evidence that the environments at the two hydrogen atoms of the water molecule are significantly different. An accurate neutron diffraction study (Tellgren, Ramanujam & Liminga, 1974) indicates that the hydrogen atoms are involved in hydrogen bonds of greatly differing strengths; the $O(W)\cdots O$ distances are 2·71 and 2·90 Å, the corresponding $H\cdots O$ distances are 1·74 and 1·95 Å (Figs. 1 and 2). This difference is also evidenced by the widely differing stretching frequencies (ν_{OH}) and quadrupole coupling constants (e^2qQ/h) observed in a combined infrared and deuteron magnetic resonance study made recently at this Institute (Berglund, Lindgren & Tegenfeldt, 1974).

A recent paper (Coppens, 1974) reviews earlier X–N difference electron-density studies, and concludes that results can be obtained which compare favourably with those from sophisticated theoretical calculations. This is further borne out in a comparitive X–N and theoretical study of α-glycine (Almlöf, Kvick & Thomas, 1973) made at this Institute. It also emerged from the Coppens survey that all previous X–N studies of *non-centrosymmetric* structures have involved an inadequate treatment of the phase problem, leading to a systematic underestimate of the difference density. In this paper the phase problem has been treated after the manner suggested by Coppens (1974); the effect of neglecting the phase problem is also demonstrated.

For comparison *ab initio* MO-LCAO-SCF calculations have been made for the formate ion and water molecule in $LiHCOO.H_2O$. Here, the electron density

* Part XCV: *Acta Univ. Upsal.* (1974). No. 322.

contribution from each constituent free ground-state atom is subtracted from the calculated electron density of the molecule. The effect of crystal field is also simulated by an appropriate distribution of point charges. A theoretical calculation was considered especially desirable for comparison purposes in the present case since the content of X–N maps for non-centrosymmetric structures must necessarily be regarded with an extra degree of scepticism.

Crystal data

Lithium formate monohydrate, $LiHCOO.H_2O$. F.W. 69·97. Orthorhombic, $Pna2_1$. General position coordinates: (x,y,z), $(-x,-y,\frac{1}{2}+z)$, $(\frac{1}{2}-x,\frac{1}{2}+y,\frac{1}{2}+z)$, $(\frac{1}{2}+x,\frac{1}{2}-y,z)$. Cell dimensions at 25 °C: $a=9{\cdot}98436\,(2)$, $b=6{\cdot}49058\,(4)$, $c=4{\cdot}85227\,(5)$ Å; $V=314{\cdot}45$ Å^3, $Z=4$. $D_x=1{\cdot}478$ g cm^{-3} (Torre, Abrahams & Bernstein, 1971).

Table 1. *Summary of X-ray and neutron refinements*

Data	$R(F)$	$R_w(F)$	Number of reflexions	Number of parameters	$\bar{\sigma}_{Y-Y}$ (Å)	$\bar{\sigma}_{Y-H}$ (Å)
X	0·033	0·041	866	57	0·001	0·024
N	0·025	0·028	424	73	0·002	0·004
X–N	0·045	0·061	866	1*		

* Scale factor on F_{obs} increased by 3·1 %.

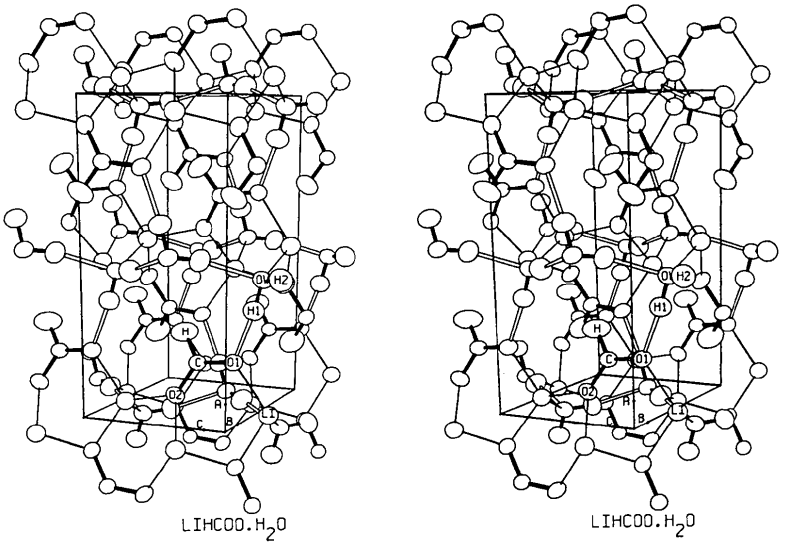

Fig. 1. A general stereoscopic view of the structure. The labelled atoms correspond to the chosen asymmetric unit. Covalent bonds: thick solid lines; H···O hydrogen-bond contacts: thick unfilled lines; electrostatic interactions: thin unbroken lines. Both here and in Fig. 2 thermal vibration ellipsoids are drawn to include 50 % probability.

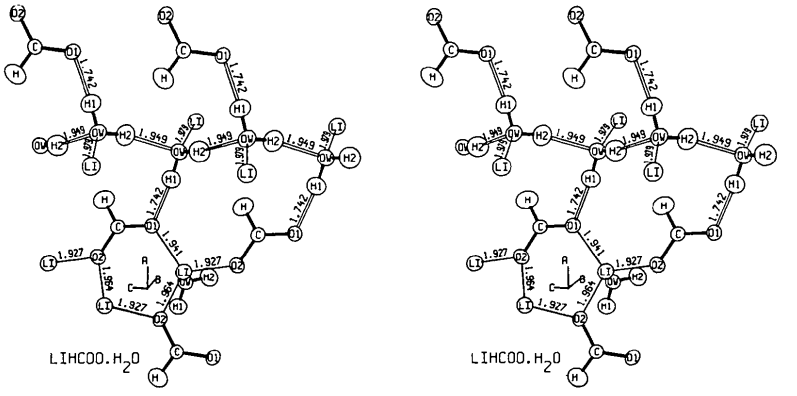

Fig. 2. A stereoscopic view of the bonding scheme in the structure as determined by neutron diffraction, viewed in the same orientation as Fig. 1.

Experimental

The neutron diffraction data were collected at ~25°C at the Studsvik R2 reactor. The study is described in detail by Tellgren *et al.* (1974); see Table 1.

The X-ray data were collected at ~25°C on a Stoe–Philips four-circle diffractometer controlled by a PDP 8/I computer and operating in an $\omega/2\theta$-scan mode. The room housing the diffractometer was humidity controlled to ~40% relative humidity. Further general details pertaining to the data collection are referred to by Thomas (1972).

All reflexions were measured within a complete octant of reciprocal space out to $\sin\theta/\lambda = 0.9046$ Å^{-1} (λ for Mo $K\alpha = 0.71069$ Å). Only small random fluctuations (up to $\pm 2.5\sigma$) were observed in the intensities of the three standard reflexions monitored throughout the data collection. The data were corrected for background, Lorentz–polarization effects and absorption. The latter correction used a crystal description made in terms of its nine rational boundary planes (Coppens, Leiserowitz & Rabinovich, 1965). The maximum dimension within the crystal was ~0·30 mm. The calculated transmission factors ranged from 0·977 to 0·985 ($\mu = 1.543$ cm^{-1}). In all, 1027 independent reflexions were collected (excluding systematic absences), of which 866 had F^2 values greater than $2\sigma(F^2)$. The latter were used in the refinement.

A full-matrix least-squares refinement of the data was made, minimizing the function $\sum w(F_o - F_c)^2$, where $w^{-1} = [\sigma^2_{\text{count}}(F^2) + (kF^2)^2]/4F^2$; the value of k in the final refinements was 0·04. Starting values for the positional parameters were taken from the neutron study; isotropic temperature factors were ascribed to the hydrogen atoms. The refined value of an isotropic extinction parameter g (see Coppens & Hamilton, 1970) was 8156 (1428). The final R values are given in Table 1.

The spherical X-ray form factor for Li^+ was taken from *International Tables for X-ray Crystallography* (1962); the form factors used for neutral oxygen and carbon were those of Hanson, Herman, Lea & Skillman (1964); and the spherical form factor used for hydrogen was given by Stewart, Davidson & Simpson (1965).

Final positional and thermal parameters from the two investigations are compared in Tables 2 and 3. The observed X-ray structure factors are given in Table 4.

Comparison of X-ray and neutron parameters

A general view of the structure is given in Fig. 1; inter- and intramolecular distances and angles from both studies are given in Table 5 along with values from another recent X-ray study (Enders-Beumer & Harkema, 1973). Some of the distances obtained from the neutron study are given in Fig. 2.

As was found in the earlier case of α-glycine (Almlöf, Kvick & Thomas, 1973), the refined X-ray and neutron positions of the non-hydrogen atoms correspond extremely closely (mean difference: 1·1σ). The largest 'shifts' [in O(W) and O(2); see Table 2] will later be seen to be associated with large asymmetric deviations from a spherical charge distribution in the immediate vicinity of the atom concerned. The hydrogen-atom positions again exhibit much larger discrepancies (mean difference: 4·1σ). A displacement of 0·133 Å for the hydrogen atom of the formate ion resembles closely the effects found for the hydrogens in the two C–H bonds of α-glycine (0·130 and 0·133 Å). This suggests some degree of constancy in the shifts of X-ray- with respect to neutron-observed hydrogen-atom positions where the hydrogen atom does not participate in hydrogen bonding. The larger differences observed in the water-hydrogen positions result from the more polar character of the charge distribution associated with an O–H bond; furthermore, the dissimilarity of these differences (0·260 and 0·199 Å for H(1) and H(2), respectively) reflects the different hydrogen-bond participation of the two hydrogen atoms.

As intimated earlier for α-glycine, the X–H directions as determined with X-rays and neutrons exhibit only small disparities. 2·9°, 3·7° and 1·4° in C–H, O(W)–H(1) and O(W)–H(2), respectively; the somewhat larger value for O(W)–H(1) can again be related to H(1)'s stronger hydrogen-bond participation. Agreement between the anisotropic thermal parameters for Li and H from the two studies is tolerably good (mean difference: 1·8σ) (Table 3). For the C and O atoms the agreement is somewhat better (mean difference: 1·3σ),

Table 2. *The neutron and X-ray atomic positional parameters* ($\times 10^4$)

For each atom the rows are, in order: neutron parameter, X-ray parameter, neutron–X-ray difference. Δ is the distance between X-ray and neutron determined positions for a given atom.

	x	y	z	Δ (Å)
Li	493 (4)	1165 (6)	−2298 (11)	0·005
	493 (2)	1160 (3)	−2290 (5)	
	0 (5)	5 (7)	−8 (12)	
H	2828 (3)	1598 (9)	3716 (10)	0·133
	2734 (21)	1603 (28)	3521 (61)	
	94 (21)	−5 (29)	195 (62)	
C	1953 (1)	1127 (2)	2542 (4)	0·003
	1954 (1)	1123 (2)	2540 (3)	
	−1 (2)	4 (3)	2 (5)	
O(1)	2081 (1)	997 (3)	0	0·002
	2080 (1)	999 (2)	0	
	1 (2)	−2 (4)	0	
O(2)	902 (1)	786 (2)	3854 (5)	0·006
	901 (1)	781 (1)	3863 (3)	
	1 (1)	5 (3)	−9 (6)	
O(W)	4656 (1)	1097 (2)	−1789 (4)	0·008
	4661 (1)	1104 (1)	−1781 (3)	
	−5 (2)	−7 (3)	−8 (5)	
H(1)	3710 (2)	1083 (4)	−1280 (7)	0·260
	3948 (23)	1048 (27)	−1489 (68)	
	238 (23)	35 (28)	209 (69)	
H(2)	4762 (3)	239 (5)	−3397 (9)	0·199
	4734 (20)	436 (26)	−3089 (53)	
	28 (20)	−197 (27)	−308 (54)	

Table 3. *Anisotropic thermal parameters* ($\times 10^4$) *observed with neutrons and X-rays*

The form of the temperature factor is $\exp[-(\beta_{11}h^2+\ldots+2\beta_{12}hk+\ldots)]$. For each atom the rows are as in Table 2. The r.m.s. components of thermal displacement ($R_i \times 10^3$ Å) along the principal axes of the thermal vibration ellipsoids are also given.

	β_{11}	β_{22}	β_{33}	β_{12}	β_{13}	β_{23}	R_1	R_2	R_3
Li	63 (3)	184 (7)	261 (18)	−7 (4)	−4 (6)	−21 (10)	170 (6)	180 (5)	202 (5)
	50 (1)	161 (3)	174 (7)	−6 (2)	9 (2)	−9 (4)	141 (3)	160 (2)	187 (2)
	13 (3)	23 (8)	87 (19)	−1 (5)	−13 (6)	−12 (11)			
H	90 (3)	626 (17)	366 (16)	−75 (5)	−28 (6)	−70 (15)	177 (4)	225 (5)	375 (5)
	62 (21)*	371 (67)	159 (99)	−52 (32)	3 (38)	−37 (86)			
	28 (22)	255 (69)	207 (100)	−23 (33)	−31 (39)	−33 (88)			
C	47 (1)	191 (3)	188 (5)	−10 (1)	−2 (2)	−11 (3)	148 (2)	154 (2)	204 (1)
	45 (1)	173 (2)	196 (3)	−8 (1)	−9 (1)	−8 (2)	143 (1)	159 (1)	194 (1)
	2 (1)	18 (4)	−8 (6)	−2 (2)	7 (3)	−3 (4)			
O(1)	47 (1)	286 (5)	187 (7)	−1 (2)	10 (2)	−5 (4)	144 (2)	160 (2)	247 (2)
	47 (1)	277 (3)	190 (3)	1 (1)	11 (1)	−2 (2)	143 (1)	161 (1)	243 (1)
	0 (1)	9 (6)	−3 (8)	−2 (3)	−1 (3)	−3 (5)			
O(2)	60 (1)	195 (3)	202 (5)	−22 (1)	20 (2)	−28 (4)	146 (2)	167 (2)	216 (2)
	59 (1)	188 (2)	188 (3)	−20 (1)	20 (1)	−25 (2)	141 (1)	166 (1)	212 (1)
	1 (1)	7 (4)	14 (6)	−2 (2)	0 (3)	−3 (5)			
O(*W*)	58 (1)	155 (3)	263 (7)	−3 (1)	16 (2)	−4 (4)	162 (2)	180 (2)	188 (2)
	52 (1)	161 (1)	255 (3)	−2 (1)	16 (1)	−6 (2)	155 (1)	179 (1)	187 (1)
	6 (1)	−6 (3)	8 (8)	−1 (2)	0 (3)	2 (5)			
H(1)	68 (2)	243 (6)	353 (13)	3 (3)	16 (5)	22 (8)	180 (4)	206 (4)	231 (4)
	152 (39)*	303 (77)	1131 (287)	163 (39)	−135 (97)	−355 (137)			
	−84 (39)	−60 (77)	−778 (288)	−160 (39)	151 (97)	377 (137)			
H(2)	93 (3)	242 (7)	375 (14)	5 (3)	19 (5)	−65 (9)	188 (5)	221 (3)	244 (4)
	57 (23)*	279 (69)	320 (148)	0 (28)	66 (43)	−105 (78)			
	36 (23)	−37 (69)	55 (148)	5 (28)	47 (43)	40 (79)			

* β-values for H, H(1) and H(2) taken from a subsequent refinement [see text and Fig. 3(*f*)]; the refined isotropic thermal parameters (*B*) were: 4·0 (4), 4·2 (5) and 3·1 (4) Å^2, respectively.

Table 4. X–N *structure factor table after scaling*

The five columns are, in order: *k*, *l*, $100|F_{obs,X}|$, $100|F_{calc,N}|$ and $\Delta\varphi$, as defined in the text. The $|F_{obs,X}|$ values are appropriate to the positional parameters given in Table 2. The reflexions 002, 120, 201 and 310 are the four most strongly extinction affected reflexions which, along with certain very weak reflexions ($|F_{obs,X}| \lesssim 0{\cdot}50$), were omitted in producing the maps shown in Fig. 3(*b*), (*c*), (*e*) and (*f*) and Fig. 4(*b*) and (*d*).

Note: this is not a conventional structure factor table.

Table 5. *Distances and angles in* $LiHCOO.H_2O$ *derived from the X-ray and neutron refinements*

The transformations inferred by the superscripts are the following:

(i) $x \quad y \quad -1+z$ (ii) $-x \quad -y \quad -\frac{1}{2}+z$
(iii) $-\frac{1}{2}+x \quad \frac{1}{2}-y \quad z$ (iv) $1-x \quad -y \quad -\frac{1}{2}+z$

(*a*) Li^+	X-ray†	X-ray	Neutron
Li·····O(1)	1·938 (4) Å	1·939 (3) Å	1·941 (5) Å
Li·····O(2^{I})	1·923 (4)	1·926 (2)	1·927 (5)
Li·····O(2^{II})	1·954 (4)	1·959 (2)	1·964 (4)
Li·····O(W^{iii})	1·974 (4)	1·975 (2)	1·979 (4)
Li·····O	1·947	1·950	1·953
O(1^{I})···Li···O(2)		112·06 (10)°	112·11 (21)°
O(1)···Li···O(2^{II})		112·46 (11)	112·30 (23)
O(1)···Li···O(W^{iii})		108·70 (10)	108·89 (22)
O(2^{I})···Li···O(2^{II})		110·18 (10)	110·12 (22)
O(2^{II})···Li···O(W^{iii})		108·97 (10)	108·96 (23)
O(2^{II})···Li···O(W^{iii})		104·11 (10)	104·10 (19)
(*b*) $HCOO^-$			
C———O(1)	1·244 (3) Å	1·242 (1) Å	1·243 (2) Å
C———O(2)	1·248 (3)	1·252 (1)	1·247 (2)
C———H	0·88 (3)	0·965 (23)	1·087 (4)
O(1)——C——O(2)	125·5 (2)°	125·64 (11)°	125·53 (14)°
H———C——O(1)	115 (2)	115·4 (1·7)	117·17 (26)
H———C——O(2)	120 (2)	118·9 (1·7)	117·30 (26)
(*c*) Hydrogen bonds			
O(*W*)···O(1)	2·715 (3) Å	2·719 (1) Å	2·714 (2) Å
O(*W*)—H(1)		0·726 (24)	0·976 (3)
H(1)····O(1)		2·001 (25)	1·742 (3)
O(*W*)—H(1)···O(1)		169·9 (3·4)°	173·63 (30)°
O(*W*)···O(W^{iv})	2·897 (3) Å	2·898 (1) Å	2·896 (2) Å
O(*W*)—H(2)		0·772 (23)	0·965 (4)
H(2)····O(W^{iv})		2·139 (24)	1·949 (4)
O(*W*)—H(2)···O(W^{iv})		167·9 (2·1)°	166·64 (28)°
[H(1)——O(*W*)—H(2)		103·0 (2·6)	107·84 (28)]

† Values given by Enders-Beumer & Harkema (1973).

but even here the disagreement is significant in certain cases [*e.g.* in $\beta_{11}(OW)$].

Calculation of the X–N *Fourier synthesis*

The difference electron density ϱ_{X-N} at a point **r** in the unit cell is given, following the notation of Coppens (1974), by the expression:

$$\varrho_{X-N}(\mathbf{r}) = \frac{1}{V} \sum_{\mathbf{H}} (\mathbf{F}_{obs,X} - \mathbf{F}_{calc,N}) \cdot \exp(-2\pi i \mathbf{H} \cdot \mathbf{r})$$

The vector $\mathbf{F}_{obs,X}$ is the observed X-ray structure amplitude with accompanying phase, and $\mathbf{F}_{calc,N}$ is the structure factor calculated using spherical free-atom X-ray scattering factors and the positional and thermal parameters derived from a neutron diffraction study. For a non-centrosymmetric structure it is clearly inadmissable to assume (as has been done in earlier X–N studies) that the phase angles associated with $\mathbf{F}_{obs,X}$ and $\mathbf{F}_{calc,N}$ are the same. Such an assumption is likely to lead to considerable errors in the difference vectors contributing to the X–N Fourier summation; see Fig. 4 and accompanying discussion in Coppens (1974). In the present study, therefore, the phases of $\mathbf{F}_{obs,X}$ are taken to be the calculated phases following the final refinement of the X-ray data. As in the case of a centrosymmetric structure, an overall scale factor was calculated between $\mathbf{F}_{obs,X}$ and $\mathbf{F}_{calc,N}$; its value (multiplying $\mathbf{F}_{obs,X}$) decreased by 3·1% with respect to the scale factor derived from the X-ray refinement. The magnitude and phase of the difference vector $(\mathbf{F}_{obs,X} - \mathbf{F}_{calc,N})$ was then calculated for each X-ray observation. The values of $|\mathbf{F}_{obs,X}|$, $|\mathbf{F}_{calc,N}|$ and the calculated phase difference ($\Delta\varphi$) are given in Table 4. The mean phase difference ($|\Delta\varphi|$) taken over all observed X-ray reflexions (except four very weak *hk*0 reflexions for which phase changes of 180° occurred) is 3·3°; whereas individual phase differences in the range 10–30° are not uncommon. The corresponding r.m.s. phase difference $(\overline{\Delta\varphi^2})^{1/2}$ is 7·2°. The resulting φ_{X-N} maps in the plane of the COO group and H_2O molecule using all X-ray observations are shown in Fig. 3(*a*) and (*d*).

Strictly, the calculation of a Fourier synthesis requires summation over *all* observations. Nevertheless, the effect on the resulting X–N maps of the joint exclusion of two types of reflexion was investigated:

(*a*) Weak reflexions whose F^2 values were less than $3\sigma(F^2)$ (217 reflexions in all).

(*b*) Strong reflexions whose F values were, following the least-squares refinement, adjudged to be more than 7% affected by extinction (four reflexions).

As a result of these exclusions the mean phase difference became 2·2° and the r.m.s. phase difference 3·4°. It should be noted that neither of these omissions would be necessary or indeed desirable in the ideal situation where a high degree of confidence can be placed in the determination of the magnitude and phase of $\mathbf{F}_{obs,X}$. It is inevitable here, however, that systematic errors can result from their inclusion in view of the inadequate treatment of vibrational motion and extinction; TDS corrections are also neglected. It was hoped that the resulting maps [Fig. 3(*b*) and (*e*)] would give a qualitatively truer picture of the difference electron density distribution.

Whilst omitting the reflexions referred to above, the effect on the appearance of the maps of two further modifications to the calculation procedure was examined: an additional half-electron scattering power was added to each of the oxygen atoms of the $HCOO^-$ ion [Fig. 3(*c*)]. The modified form factor $f(O^{1/2-})$ was calculated from the expression: $f(O^{1/2-}) = [f(O) + f(O^-)]/2$. The $f(O)$ and $f(O^-)$ values were here taken from *International Tables for X-ray Crystallography* (1962).

In the preparation of a further map [Fig. 3(*f*)] anisotropic temperature factors (β_{ij}'s) were used instead of isotropic (B's) for the hydrogen atoms in the X-ray refinement, the intention being to ascertain the extent to which the appearance of the difference maps in the vicinity of hydrogen atoms would be affected by the use of B(H)'s in the X-ray refinement.

In a final series of maps (Fig. 4) the effect is demonstrated of totally ignoring the phase problem (*i.e.* assuming $A\varphi=0$ for all reflexions).*

Quantum-mechanical calculations

Separate *ab initio* MO-LCAO-SCF calculations were made for the $HCOO^-$ ion and H_2O molecule as they arise in the $LiHCOO.H_2O$ structure, using the program system MOLECULE (Almlöf, 1972).

The basis set used comprised basis functions (θ_i's) which are linear combinations of single Gaussians, *i.e.*

$$\theta_i = N_i x^{\mu_i} y^{\nu_i} z^{\omega_i} \sum_j a_{ij} \exp(-\alpha_{ij} r^2)$$

where N_i is a normalization constant and the factor $x^{\mu_i}y^{\nu_i}z^{\omega_i}$ denotes the type ($s,p,d,\ldots$) of the basis function. The a and α values used for carbon and oxygen were those given by Dunning (1970), with nine *s*- and five groups of *p*-type Gaussians on each atom centre. These were contracted to four *s*- and two *p*-type functions. In addition, one group of *d*-type polarization functions was included for each atom, with exponents 1·3 and 0·6 for oxygen and carbon, respectively. The basis set used for hydrogen was that given by Huzinaga (1965), involving four *s*-type Gaussians contracted to two and a group of *p*-type functions with exponents 0·8.

The electrostatic fields imposed on the $HCOO^-$ ion and H_2O molecule by their respective crystal environments were simulated following a technique described by Almlöf & Wahlgren (1973). The fields from an infinite crystal were calculated by assigning point charges to the neutron-determined atom positions; the magnitudes of the charges were those obtained from a population analysis for the free $HCOO^-$ ion and H_2O molecule. These fields were then each reproduced by a set of ~ 50 point charges placed at the neutron-determined nearest-neighbour positions. The values of these charges were arrived at by a least-squares procedure.

The difference electron density was obtained by firs:

* For brevity, maps in Figs. 3 and 7, are referred to as having been prepared by the *non-centrosymmetric treatment*; maps in Fig. 4 by the *centrosymmetric treatment*.

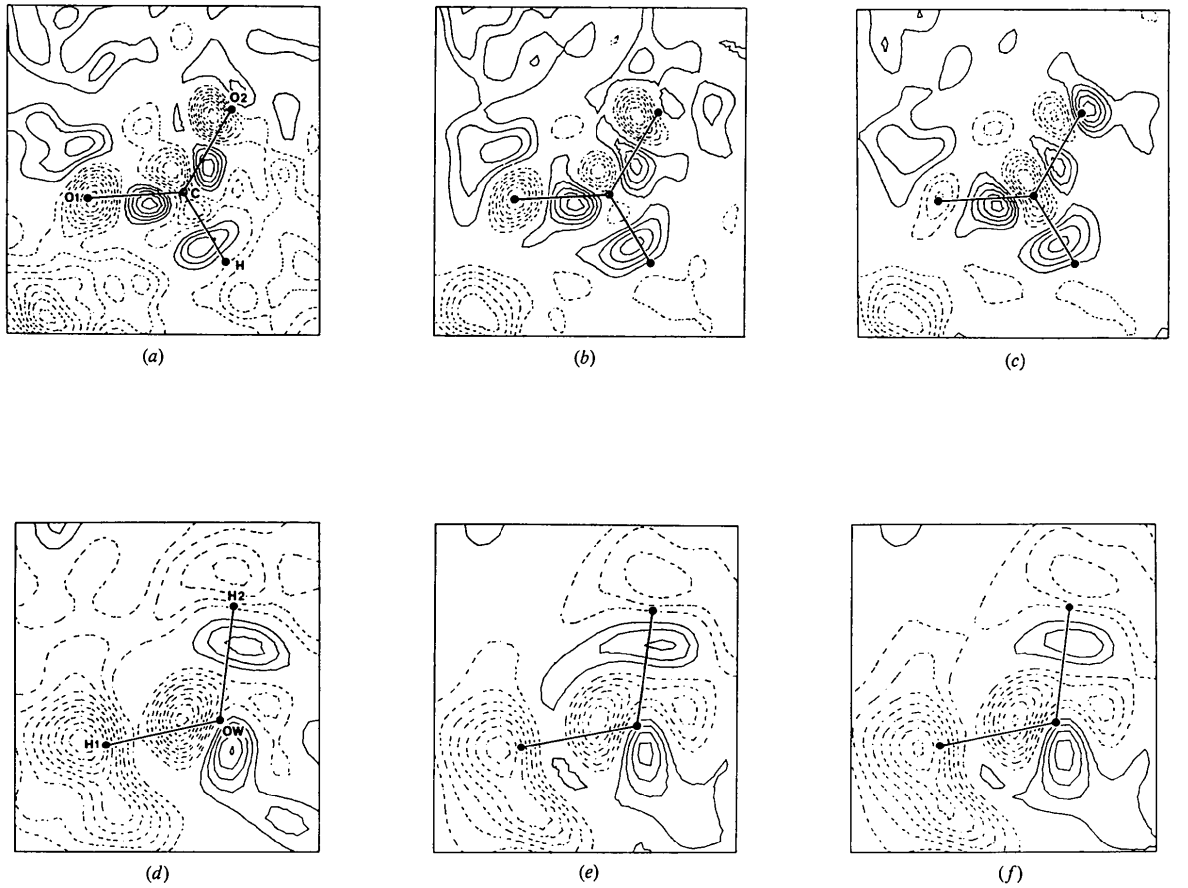

Fig. 3. X–N difference electron density maps for the $HCOO^-$ ion (*a–c*) and H_2O molecule (*d–f*) in $LiHCOO.H_2O$, calculated taking account of phase differences between $F_{obs,X}$ and $F_{calc,N}$ which arise since the structure is non-centrosymmetric. See text for details of the calculation. Contours are drawn at intervals of 0·05 e $Å^{-3}$; regions of electron excess are indicated by unbroken lines. The zero-level contour has been omitted.

calculating the electron densities for the $HCOO^-$ ion and H_2O molecule in the simulated crystal field, and from these subtracting the atomic electron densities calculated for the free component atoms in their ground states using the *same* basis set. The resulting difference maps in the COO and H_2O planes are given in Fig. 5. The calculated difference electron density between the H_2O molecule in the crystal field and a free H_2O molecule is given in Fig. 6.

All quantum-mechanical calculations were made on the CDC 3600 computer at the Physics Department of the University of Stockholm; the remaining calculations were made at the Uppsala Data Center on an IBM 370/155 computer.

Discussion

General comments on the X–N *difference maps*

Inspection of Figs. 3 and 4 reveals a number of points of more general relevance:

(*a*) Comparing the centro- and non-centrosymmetric treatments, we see that both result in maps containing the *same general features* but with an overall tendency towards a weakening of 'peak intensities' in the centrosymmetric case. Noticeable also, however, is that the centrosymmetric H_2O maps [Fig. 4(*c*) and (*d*)] agree less well with their non-centrosymmetric counterparts than do the $HCOO^-$ maps. This is especially evident in the region of O(*W*) and illustrates the point that, for a non-centrosymmetric structure, certain X–N sections can be more sensitive than others to a neglect of the phase problem. In the present case the *c*-projection is centrosymmetric, making $\Delta\varphi$ for *hk*0-type reflexions necessarily 0° or 180° (Table 4).

(*b*) If we consider the more rigorous non-centrosymmetric treatment (Fig. 3), it is instructive to note the effect of omitting weak and strongly extinction affected reflexions from the synthesis. In both sections the level of noise would appear to be reduced by

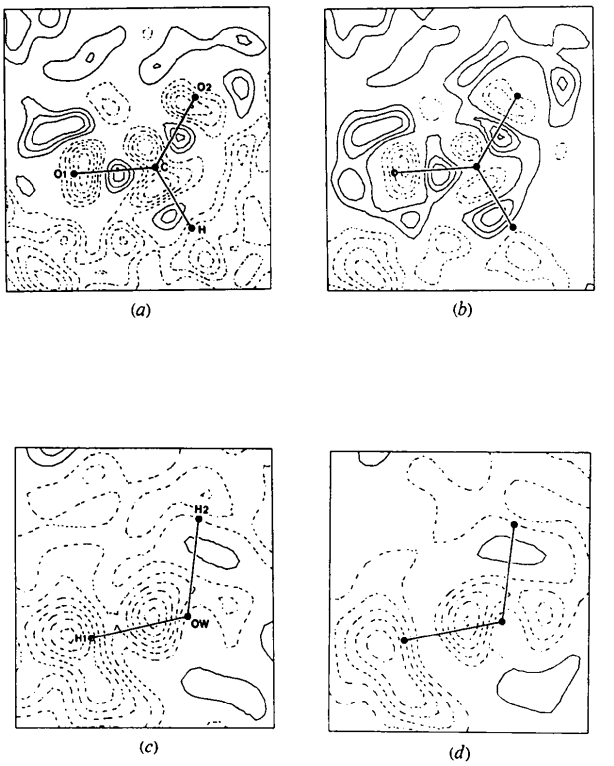

Fig. 4. X–N difference electron density maps for the $HCOO^-$ ion (*a* and *b*) and H_2O molecule (*c* and *d*) in $LiHCOO.H_2O$, calculated while neglecting the phase problem [*cf.* Fig. 3(*a*), (*b*), (*d*), (*e*)]. See text for details of calculation. Contours drawn as in Fig. 3.

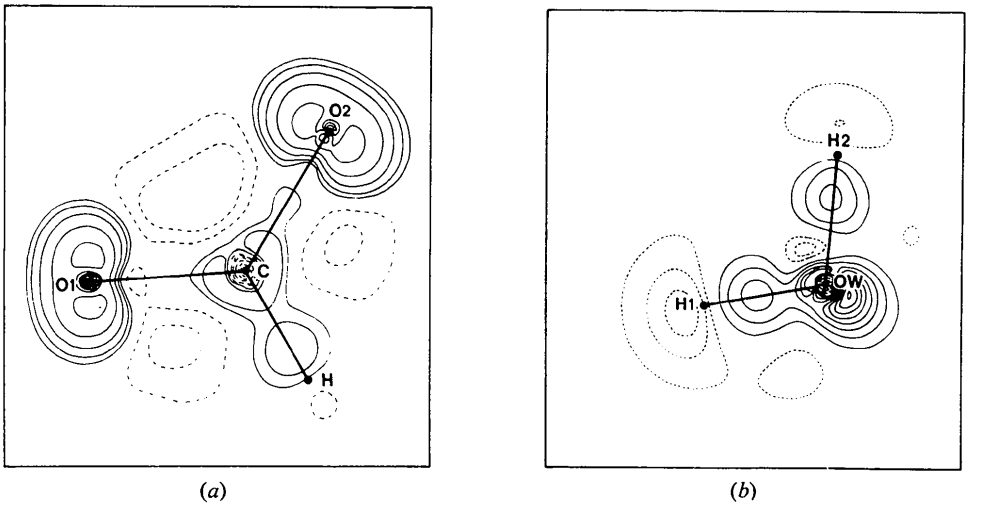

Fig. 5. Theoretical difference electron density maps for (*a*) the $HCOO^-$ ion, and (*b*) the H_2O molecule in $LiHCOO.H_2O$. Contours are drawn at intervals of 0·10 e $Å^{-3}$; regions of electron excess are indicated by unbroken lines. The zero-level contour has been omitted.

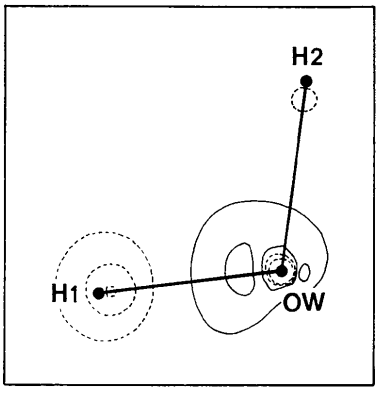

Fig. 6. Theoretical difference electron density between the H_2O molecule in a simulated crystal field and the free molecule. Contours drawn as in Fig. 5.

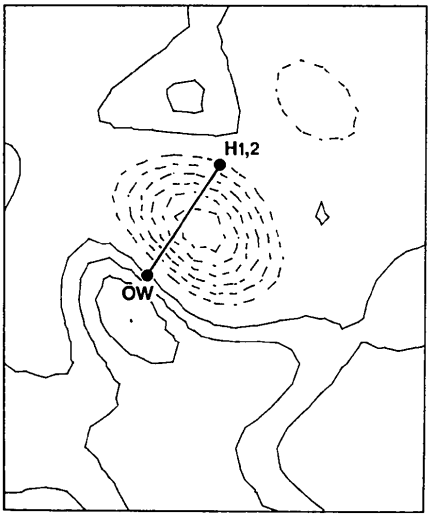

Fig. 7. X–N difference electron density map in the plane perpendicular to the plane of the H_2O molecule, passing through the water-oxygen atom and the mid-point between H(1) and H(2). The map is prepared using the non-centrosymmetric treatment and the contours are drawn as in Fig. 3.

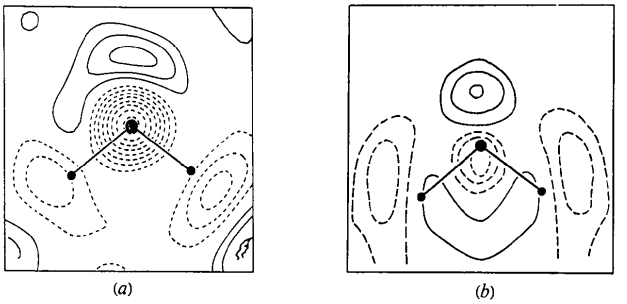

Fig. 8. Earlier X–N difference electron density maps for D_2O molecules in (*a*) α-$(COOD)_2.2D_2O$ and (*b*) $(ND_4)_2C_2O_4.D_2O$. The figures are reproduced with minor modification from Coppens *et al.* (1969) and Taylor & Sabine (1972), respectively. The contours are drawn as in Fig. 3.

$\sim 0{\cdot}05$ e Å^{-3}, while at the same time the peak heights are only trivially affected. Inspection of apparently 'meaningless' regions would suggest a standard deviation of 0·05–0·10 e Å^{-3}. An omission procedure is thus proposed as a useful practical safeguard, particularly in the calculation of X–N maps for non-centrosymmetric structures, with the obvious warning that the integrity of quantitative information contained in the maps can be jeopardized. Appropriate omission criteria must naturally be assessed for each individual case.

(*c*) In Fig. 3(*c*) an attempt has been made to equip the oxygen atoms of the $HCOO^-$ ion with a potentially more realistic X-ray form factor in the hope of better resolving the non-spherical components of the difference electron density. This procedure would appear to induce a net movement of electron density *towards* the oxygen sites and away from the carbon site. On the other hand, no tendency is observed for any sharpening of the features associated with the lone-pair sites of the oxygen atoms. It is unlikely that these observations have any real significance, but rather illustrate the inherent practical difficulty of detecting non-spherical features in the charge density when the appropriate spherical atomic form factor is in question. The effect of using a 'wrong' form factor can easily swamp genuine difference electron-density effects. For this reason, Fig. 3(*b*) is taken as a more plausible representation of the true situation.

(*d*) It is conceivable that certain of the features of the H_2O maps, *e.g.* Fig. 3(*e*), could follow from the use of isotropic temperature factors for the hydrogen atoms in the X-ray refinement. The map shown in Fig. 3(*f*) is an attempt therefore to investigate this, and results from the use of anisotropic temperature factors for all hydrogen atoms (see Table 3). It is seen, however, that this modification brings about the most trivial of changes to the map shown in Fig. 3(*e*).

It is therefore felt that the most credible maps are those appearing in Fig. 3(*b*) and (*e*), the contents of which will now be discussed and compared with the results from the *ab initio* calculations.

The $HCOO^-$ *ion*: X–N *map*

Though not a requirement of symmetry, an approximate mirror plane appears perpendicular to the plane of the ion and passing through the C–H bond. This is not unexpected in view of the geometrical symmetry of the ion, and serves as an internal check on the reliability of the method. The maximum bonding charge densities in the C–O bonds of 0·22 and 0·28 e Å^{-3} compare with mean values of $\sim 0{\cdot}22$ e Å^{-3} in α-glycine (Almlöf, Kvick & Thomas, 1973) and $\sim 0{\cdot}20$ e Å^{-3} in α-deutero-oxalic acid dihydrate (Coppens, Sabine, Delaplane & Ibers, 1969). The peak polarization charge density in the C–H bond is 0·23 e Å^{-3} compared with values of $\sim 0{\cdot}29$ and $\sim 0{\cdot}31$ e Å^{-3} in α-glycine. It will also be observed that regions of electron deficiency appear near the terminal oxygen

sites; this is a result common to all previous X–N observations of oxygen atoms in this type of situation. A further interesting feature relates to the lone-pair sites of O(1) and O(2). No electron density is observed associated with O(1) in the direction of acceptance of the stronger hydrogen bond O(*W*)–H(1)···O(1) (Fig. 2). Moreover, only relatively weak concentrations of electron density (peak heights ~0·15 e Å^{-3}) are observed at the three remaining lone-pair sites (assuming an sp^2 hybridization scheme), all of which lie roughly in the direction of O···Li$^+$ electrostatic interactions.

The $HCOO^-$ *ion: ab initio calculation*

Few of the above observations are reproduced by the quantum mechanical *ab initio* calculations [see Fig. 5(*a*)]. A certain correspondence is found in the general form of the difference charge density associated with the polarization of the hydrogen atom, and in the approximate mirror symmetry in the maps. A suggestion of C–O bonding charge density is also discernible in the *ab initio* map but the associated maxima lie disturbingly near the carbon atom. It is in the region of the oxygen atoms that the disagreement with experiment is at its most serious, however. The *ab initio* treatment produced two equally strong peaks for each oxygen, with their maxima lying in directions at right angles to the C–O bonds. This bears little relation to the much weaker and unequally developed peaks found in the X–N map at positions predicted on the basis of an sp^2 hybridization scheme. That the calculated peaks are more intense is, in itself, not so surprising since the *ab initio* procedure takes no account of the smearing effect produced by thermal motion (*cf.* Coppens, 1974). Nevertheless, the general agreement with experiment is poor in this case.

The water molecule: X–N *map*

In contrast to the case of the $HCOO^-$ ion, the difference electron density in the water molecule [Fig. 3(*e*)] exhibits a marked asymmetry. The situation in the region of H(2) has the classical appearance of a hydrogen atom polarized by the heavy atom to which it is covalently attached, *i.e.* a region of electron density on the heavy-atom side of the proton (peak height here ~0·15 e Å^{-3}), and a region of electron deficiency on its opposite side. Similar polarization features are also apparent for H(1) but it is also evident that the whole region around H(1) has suffered an *overall loss* of charge, the electron density nowhere being greater than that for the isolated atoms. It is significant that H(1) participates in a relatively strong (2·71 Å) hydrogen bond, whereas H(2) is engaged in a much weaker (2·90 Å) hydrogen bond.

The difference electron density associated with the lone-pair sites on O(*W*) is also grossly asymmetric both in the H_2O plane and in the perpendicular plane bisecting the H–O–H angle (Fig. 7). Only one lobe is developed (peak height 0·22 e Å^{-3}, compared to 0·17 e Å^{-3} in the two earlier X–N studies of the water molecule discussed below) roughly in the direction of hydrogen-bond acceptance from H(2).

A final point worth noting in relation to the experimental difference maps for the water molecule is the pronounced dominance of electron deficient regions in both Fig. 3(*e*) and Fig. 7. This might suggest that the water molecule as a whole has suffered a loss of charge amounting to several tenths of an electron, and would seem to support arguments promoting the importance of the role of charge transfer in hydrogen bonding. A severe note of warning, however: the zero-level in the maps is highly sensitive to the scale factor used between $\mathbf{F}_{obs,X}$ and $\mathbf{F}_{calc,N}$. No experimental determination of this quantity has been made here, however, and its calculated value must necessarily be viewed with mistrust. This fact clearly prejudices a direct comparison of experimental and theoretical difference maps.

At this point it is relevant to compare the present map with those from earlier X–N studies of hydrates. The map published for α-deutero-oxalic acid dihydrate (Coppens, Sabine, Delaplane & Ibers, 1969) [Fig. 8(*a*)] was calculated without previously scaling $\mathbf{F}_{calc,N}$ to $\mathbf{F}_{obs,X}$. It is dominated by a deep trough at the position of the oxygen atom which might well disappear wholly or partially after scaling. Otherwise the map displays a high degree of symmetry, reflecting the close similarity in the lengths of the two hydrogen bonds donated by the water molecule, 2·88 and 2·91 Å (corresponding H···O distances: 1·94 and 2·01 Å). In the case of deutero-ammonium oxalate monohydrate (Taylor & Sabine, 1972) [Fig. 8(*b*)], the water molecule lies on a twofold axis which imposes a mirror symmetry on the X–N map. It will be noted, however, that the general features of the map have much in common with a 'mirror-symmetrization' of Fig. 3(*e*). The point should also be made that the map for the non-centrosymmetric structure $(ND_4)_2C_2O_4.D_2O$ was prepared while neglecting the phase problem (*i.e.* assuming $\Delta\varphi = 0°$). As demonstrated earlier, this is unlikely to effect the general features in the resulting map.

The water molecule: ab initio calculation

It is gratifying to note that the *ab initio* calculation for the water molecule [Fig. 5(*b*)] confirms the asymmetry in the difference electron density. The region around H(2) has a distinct excess of electrons over the region around H(1), indicating a net migration of charge from the hydrogen atom in the stronger bond. With the exception of the region near the nucleus (generally the most unreliable in quantum mechanical calculations), a crude qualitative correspondence with experiment can also be observed around the water oxygen atom.

It is not intuitively clear, however, to what extent the theoretical difference maps arrived at in Fig. 5 are affected by the simulated crystal environment. A density map portraying solely the effect of the external polarization was therefore computed for the water

molecule (Fig. 6). The map shows the difference between the density calculated assuming an external field and that for a free molecule. The most striking feature of the map is the additional polarization induced by the crystal field in the region of H(1). It is evident that Fig. 5(*b*) describes not only the covalent bonding situation within the molecule, but is also substantially affected by intermolecular interactions.

It would therefore seem appropriate to recommend a due measure of caution when comparing experimental and theoretical difference maps. Substantial disagreement can generally be anticipated if the polarization brought about by the environment is not properly accounted for, especially for molecules with a high polarizability and/or a markedly polar environment (*e.g.* a hydrogen-bonded situation). In more strongly hydrogen-bonded systems a purely electrostatic description of the crystal field (as employed here) will certainly prove inadequate in reproducing the experimental findings.

Some final comments

In the present work several possible sources of error exist to explain the discrepancies between the experimental and theoretical difference maps. The numerous approximations made in the preparation of X–N maps (neglect of TDS, higher cumulants, *etc.*) are especially serious in the present case of a non-centrosymmetric structure. In making the *ab initio* calculations, the description of the comparatively strong O(*W*)–H(1)$\cdots$O(1) hydrogen bond using a purely electrostatic model is clearly a crude approximation (as discussed above), especially since the entire negative charge on the acceptor atom is treated as if it were concentrated at its nucleus. It has also been demonstrated earlier (Cade, 1972) that the size of the LCAO basis set used has a crucial bearing on the form of the resulting calculated difference map. In the present calculations the valence regions can be expected to be described quite adequately (using split-shell basis + polarization functions). It can be supposed that the inherent inaccuracies in the core orbitals, following from the use of a Gaussian basis, are cancelled out by the subtraction of similarly inaccurate atomic densities. Insufficient is known about this subject at the present time for any definitive statements to be made concerning the adequacy of the basis set used. It would seem likely, however, that at least a correct qualitative picture of the charge migration will emerge – if this is at all possible within the Hartree–Fock approximation.

The authors appreciate the contribution of Professor Ivar Olovsson to this work, and also the generous assistance of the academic and technical staff of the Hydrogen Bond Group.

This work has been supported by grants from the Tricentennial Fund of the Bank of Sweden and the Swedish Natural Science Research Council; both are hereby gratefully acknowledged.

References

ALMLÖF, J. (1972). USIP Report 72-09, Univ. of Stockholm.

ALMLÖF, J., KVICK, Å. & THOMAS, J. O. (1973). *J. Chem. Phys.* **59**, 3901–3906.

ALMLÖF, J. & WAHLGREN, U. (1973). *Theor. Chim. Acta*, **28**, 161–168.

BERGLUND, B., LINDGREN, J. & TEGENFELDT, J. (1974). *J. Mol. Struct.* **21**, 135–148.

CADE, P. E. (1972). *Trans. A.C.A.* **8**, 1–36.

COPPENS, P. (1974). *Acta Cryst.* B**30**, 255–261.

COPPENS, P. & HAMILTON, W. C. (1970). *Acta Cryst.* A**26**, 71–83.

COPPENS, P., LEISEROWITZ, L. & RABINOVICH, D. (1965). *Acta Cryst.* **18**, 1035–1038.

COPPENS, P., SABINE, T. M., DELAPLANE, R. G. & IBERS, J. A. (1969). *Acta Cryst.* B**25**, 2451–2458.

DUNNING, T. H. (1970). *J. Chem. Phys.* **53**, 2823–2833.

ENDERS-BEUMER, A. & HARKEMA, S. (1973). *Acta Cryst.* B**29**, 682–685.

HANSON, H. P., HERMAN, F., LEA, J. D. & SKILLMAN, S. (1964). *Acta Cryst.* **17**, 1040–1044.

HUZINAGA, S. (1965). *J. Chem. Phys.* **42**, 1293–1302.

International Tables for X-ray Crystallography (1962). Vol. III. Birmingham: Kynoch Press.

STEWART, R. F., DAVIDSON, E. R. & SIMPSON, W. T. (1965). *J. Chem. Phys.* **42**, 3175–3187.

TAYLOR, J. C. & SABINE, T. M. (1972). *Acta Cryst.* B**28**, 3340–3351.

TELLGREN, R., RAMANUJAM, P. S. & LIMINGA, R. (1974). *Ferroelectrics*, **6**, 191–196.

THOMAS, J. O. (1972). *Acta Cryst.* B**28**, 2037–2045.

TORRE, L. P., ABRAHAMS, S. C. & BERNSTEIN, J. L. (1971). A.C.A. Summer Meeting, M6, p. 94.